

# Self-polarization effect in the middle point of an optical fiber

A. Fusaro<sup>1</sup>, N. Berti<sup>1</sup>, M. Guasoni<sup>2</sup>, H. R. Jauslin<sup>1</sup>, A. Picozzi<sup>1</sup>, J. Fatome<sup>1</sup>, and D. Sugny<sup>1\*</sup>

<sup>1</sup> *Laboratoire Interdisciplinaire Carnot de Bourgogne (ICB),*

*UMR 6303 CNRS-Université de Bourgogne- Franche Comté,*

*9 Av. A. Savary, BP 47 870, F-21078 DIJON Cedex, FRANCE and*

<sup>2</sup> *Optoelectronics Research Centre, University of Southampton, SO17 1BJ, United Kingdom*

(Dated: May 24, 2019)

In this study, we report both numerically and experimentally an unexpected phenomenon of self-polarization occurring in the middle point of an isotropic optical fiber when two uncorrelated partially polarized waves are simultaneously injected at the ends of the fiber. More precisely, we demonstrate that two counterpropagating waves of equal intensity exhibit a spontaneous organization of their polarization states around two pools of attraction just in the middle-point of propagation, and then both recover a partially polarized state at their respective fiber outputs. The self-polarization effect then remains hidden within the optical fiber in the sense that no apparent sign of this process is detected at the fiber outputs. A geometric definition of the degree of polarization is used to measure the efficiency of the polarization phenomenon.

## I. INTRODUCTION

Understanding the mechanisms responsible for self-organization processes in conservative and reversible Hamiltonian wave systems is an arduous problem that generated significant interest. Contrary to dissipative systems that exhibit attractors, a conservative Hamiltonian system cannot evolve towards a fully ordered state, because such an evolution would imply a loss of statistical information that would violate its formal reversibility as well as the rules of entropy growth. Nevertheless, beyond this fundamental rule of thumb, a nonintegrable Hamiltonian wave system can exhibit an irreversible process of self-organization that results from its natural thermalization towards the ('most disordered') thermodynamic equilibrium state [1]. This may appear to be counterintuitive since the same mechanism, the increase of disorder or entropy, would be also responsible for a seemingly opposite phenomenon, namely the formation of large-scale coherent structures. However, it is important to note that this kind of self-organization process has in essence a thermodynamic origin, in the sense that an increase of disorder (entropy) also requires the formation of a large-scale coherent structure. Indeed, it is thermodynamically advantageous for the waves to generate a large-scale coherent or ordered structure, because this allows an increase of the amount of disorder in all the remaining surrounding landscape [1–3].

In this study, we address a different form of self-organization process that occurs in an 'open' system of interacting Hamiltonian waves. The system is 'open' in the sense that the nonlinear medium is characterized by a *finite spatial extension*. As opposed to the self-organization processes discussed above for 'closed' systems, here the waves can enter or exit the nonlinear medium, although the interaction still remains lo-

cally Hamiltonian inside the medium. In this work, the finite-length nonlinear medium consists of a piece of optical fiber of 200m long, and we study the polarization dynamics of two counter-propagating partially polarized signals that are injected at both ends of the fiber.

The polarization dynamics of counter-propagating optical beams has been widely studied in the past in different configurations [4–8], since the pioneering studies in nonlinear atomic vapors [4]. In this framework, different processes of polarization attractions have been identified depending on the type of the considered optical fiber (isotropic fiber [9–14], highly [15, 16], weakly [17] or randomly birefringent fiber [14, 18–25]). In these previous studies, polarization attraction is known to require the injection of a fully polarized (pump) wave, which serves as a state of polarization (SOP) reference, and thus plays the natural role of attractor for an arbitrary polarized backward signal beam. Subsequently, polarization attraction has been demonstrated in a single feedback mirror configuration [26–28], so that the injected wave interacts with its own back-reflected wave, thus forming a feedback loop. Note that, aside from polarization attraction, this single mirror feedback scheme can be considered as a fundamental system for the study of spontaneous pattern formation when transverse effects are considered, see e.g. [29, 30].

In this study, we report a previously unrevealed consequence of such a phenomenon of polarization self-organization. In contrast with the previous studies which require either the injection of a fully polarized reference pump wave, or the presence of a feedback mirror to introduce a correlation between the backward waves [26, 28], here, two independent random waves characterized by uncorrelated polarization fluctuations are injected at the ends of the fiber. In this way, we identify a new process of polarization self-organization that unexpectedly occurs just in the middle point of an optical fiber: As the two random waves counter-propagate through the fiber, they are first attracted towards a specific SOP in the middle of the fiber, and then both recover their polarization ran-

---

\*Electronic address: dominique.sugny@u-bourgogne.fr

domness at their corresponding fiber outputs. It turns out that, in a loose sense, this self-polarization process is ‘hidden’ within the optical fiber since no apparent sign of this phenomenon is detected in the outputs, a peculiar feature that may explain why this intriguing effect remained unrecognized so far. We introduce a geometric definition of the degree of polarization to measure the efficiency of the polarization process. As discussed below, a standard definition based on a temporal average of the time dependent polarization cannot unveil the polarization effect and leads to a vanishing measure all along the fiber.

The paper is organized as follows. The model system is introduced in Sec. II. A complete numerical analysis of the self-polarization effect is provided in Sec. III. This effect is shown experimentally in Sec. IV. Conclusion and perspective views are given in Sec. V.

## II. THE MODEL SYSTEM

The evolution of the SOP of the forward and backward propagating beams in an isotropic fiber (IF) is governed by the coupled differential equations [7, 9]:

$$\begin{cases} \frac{\partial \vec{S}}{\partial \tau} + \frac{\partial \vec{S}}{\partial \xi} = [\vec{S} \times \mathcal{I}_s \vec{S} + 2\vec{S} \times \mathcal{I}_i \vec{J}], \\ \frac{\partial \vec{J}}{\partial \tau} - \frac{\partial \vec{J}}{\partial \xi} = [\vec{J} \times \mathcal{I}_s \vec{J} + 2\vec{J} \times \mathcal{I}_i \vec{S}], \end{cases} \quad (1)$$

where  $\vec{S}$  and  $\vec{J}$  represent respectively the Stokes vectors of the forward and backward beams, with the diagonal matrix  $\mathcal{I}_s = \text{diag}(-1, -1, 0)$  and  $\mathcal{I}_i = \text{diag}(-2, -2, 0)$ , the sign  $\times$  denotes the vector product. Equations (1) are normalized with respect to the nonlinear time  $\tau_0 = 1/(\gamma v S_0)$  and nonlinear length  $\Lambda_0 = v\tau_0$ , where  $\gamma$  is the nonlinear Kerr coefficient,  $v$  the group velocity of the waves and  $S_0$  the power of the forward beam. In this paper, we use the convention in which the north and south poles of the Poincaré sphere correspond respectively to the left and right circular SOP. No fiber loss has been taken into account in the model.

We consider two partially polarized fields characterized by the boundary conditions  $\vec{S}(\xi = 0, \tau)$  and  $\vec{J}(\xi = L, \tau)$  that are injected at the ends of the fiber of normalized length  $L$ . We investigate the SOPs  $\vec{S}(\xi = L/2, \tau)$  and  $\vec{J}(\xi = L/2, \tau)$  of the two beams in the middle of this fiber. The partially polarized beams are defined by a signal wave whose SOP evolves and fluctuates over the surface of the Poincaré sphere with a coherence time  $\tau_c$ . We generate numerically the fields by considering uncorrelated complex time-dependent random functions  $A_{x,y}^{S,J}(\tau)$ , where  $A_{x,y}^S(\tau)$  ( $A_{x,y}^J(\tau)$ ) denote the linear polarizations components of the forward (backward) field. To simplify the discussion, we assume that the forward and backward fields have the same correlation time  $\tau_c$ . The random waves are generated numerically from a Gaussian-shaped

power spectrum with  $1/e^2$  half-width  $\sigma_\nu$  and with uncorrelated random spectral phases ( $\tau_c = \sqrt{\log(2)}/(\pi\sigma_\nu)$ ). Since the goal is to study the incoherent polarization dynamics, the random fields  $A_{x,y}^{S,J}$  expressed in the Stokes basis are normalized with respect to their power intensity ( $S_0$  and  $J_0$ ), i.e., the Stokes vectors  $(\vec{S}, \vec{J})$  exhibit a random motion over the surface of the corresponding Poincaré spheres of constant radii  $S_0$  and  $J_0$  ( $S_0 = J_0 = 1$  in normalized units).

## III. NUMERICAL ANALYSIS OF THE SELF-POLARIZATION EFFECT

The phenomenon of self-polarization manifests itself by the spontaneous polarization of the optical beams in the middle of the fiber, at  $\xi = L/2$ . We stress the fact that the injected partially polarized beams are uncorrelated with each other. In other words, the two waves self-organize their own SP in the middle point of an optical fiber without any reference nor feedback system. This configuration clearly represents a non trivial extension of the Omnipolarizer device reported in [26]. The self-polarization effect is illustrated by the numerical simulations of the spatio-temporal dynamics (1) reported in Fig. 1. We inject at the ends of a fiber of length 200 m ( $= 4\Lambda_0$ ) a wave with a coherence time of  $\tau_c \simeq 60 \mu\text{s}$ , which places our study in a quasi-stationary regime. As illustrated in Fig. 1, the incoherent polarization dynamics are deeply modified by the nonlinear interaction: While the injected SOPs fluctuate all over the Poincaré spheres, the SOPs in the middle of the fiber are attracted toward the poles of the spheres, which correspond to the circular polarization states of the fields.

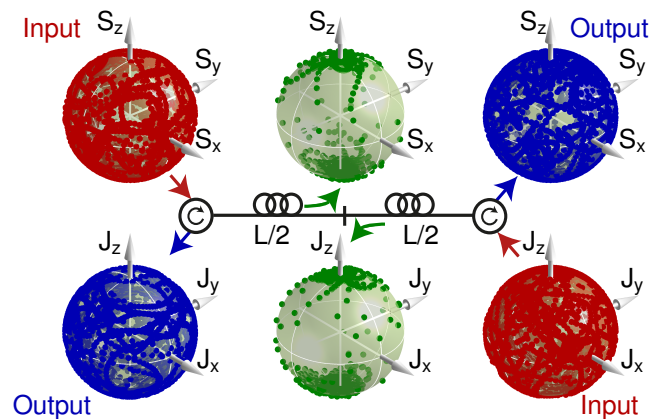


FIG. 1: (Color online) Numerical simulations of the spatiotemporal system on the Poincaré sphere. The red (gray), green (light gray) and blue (dark gray) dots denote respectively the input, middle and output SOPs of the signal ( $\vec{S}$ , upper panels) and of the pump ( $\vec{J}$ , lower panels).

We explore now the efficiency of this polarization effect with respect to the coherence time  $\tau_c$ .

To assess the strength of the polarization phenomenon, we consider the degree of polarization (DOP). Note however that the standard definition  $\text{DOP} = \sqrt{\langle S_x \rangle^2 + \langle S_y \rangle^2 + \langle S_z \rangle^2} / \langle S_0 \rangle$ , where  $\langle \cdot \rangle$  is a temporal average, is not relevant here, since it is inherently unable to unveil the polarization effect, i.e., it would lead to a vanishing DOP all along the fiber. It is more convenient to resort to a geometric definition  $\text{GDOP} = 1 - \frac{\mathcal{A}}{4\pi}$ , where  $\mathcal{A}$  is the area covered over the surface of the Poincaré sphere [31]. This geometric approach also proves relevant for quantum optics developments [32]. In the case of a completely polarized (unpolarized) field, the area is  $\mathcal{A} = 0$  ( $\mathcal{A} = 4\pi$ ) so that  $\text{GDOP} = 1$  (resp.  $\text{GDOP} = 0$ ). We present in Fig. 2 the evolution of the GDOP of the forward beam along the fiber and its variation with respect to the coherence time at  $\xi = 0$  and  $\xi = L/2$ . The same results are obtained for the backward wave. A strong increase of the GDOP is observed in the middle of the fiber in Fig. 2a. Note the smooth evolution of the GDOP along the fiber. In particular, the maximum GDOP is reached not only at  $\xi = L/2$ , but also for significant displacements around this position. As shown in Fig. 2a and b, the DOP increases as the coherence time  $\tau_c$  becomes larger. We observe that the GDOP tends to saturate for coherence times larger than  $60 \mu\text{s}$ , i.e., in the quasi-stationary regime. This represents a limit for an efficient process of self-polarization. Indeed, since the polarization effect results from the backward propagation dynamics in the fiber length  $L$ , the required minimum coherence time is naturally connected to the propagation time throughout the fiber ( $2 \mu\text{s}$  in this example), a feature that was already noticed for a standard configuration in which the pump beam is fully polarized [20].

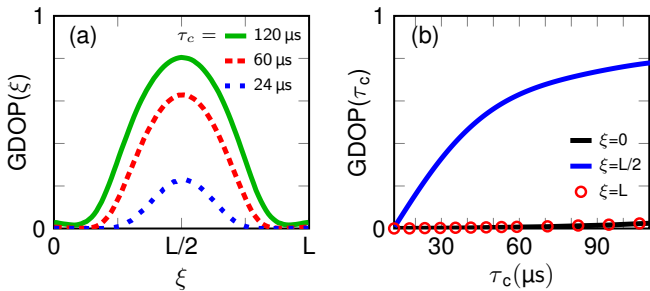


FIG. 2: (Color online) Panel (a): Evolution of the DOP as a function of the position  $\xi$  for  $\tau_c = 24 \mu\text{s}$  (blue dotted line),  $\tau_c = 60 \mu\text{s}$  (red dashed line) and  $\tau_c = 120 \mu\text{s}$  (green solid line). Panel (b): DOP of the forward beam at  $\xi = 0$  (black line),  $\xi = L/2$  (blue line) and  $\xi = L$  (red circle). The same fiber parameters as in Fig. 1 are used.

We have also studied the distribution of the fluctuations of the SOPs by computing the probability density function (PDF) for each component at a given position  $\xi$ . We see in Fig. 3 that at the fiber ends  $\xi = 0$  and  $\xi = L$  the PDFs of the three components are homoge-

neous. In marked contrast, the probability distributions exhibit a significant tightening nearby the middle of the fiber  $\xi = L/2$ : While the PDFs of  $S_x$  and  $S_y$  decrease toward zero, the PDF of the circular SOP  $S_z$  increases significantly and saturates to nearby the two extreme values  $\pm 1$  ( $\pm S_0$  in dimensional units). This analysis provides another signature of the efficiency of the polarization effect toward the circular polarization components.

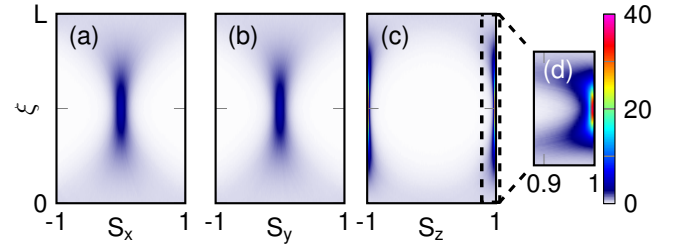


FIG. 3: (Color online) Evolution of the PDF of the three components ( $S_x, S_y, S_z$ ) of the SOP of the forward beam in panels (a), (b) and (c) as a function of the position  $\xi$ . The PDFs have been computed from the results displayed in Fig. 1. The coherence time is set to  $60 \mu\text{s}$ . Panel (d) is a zoom of panel (c).

This self-organization process can be explained through the properties of stationary solutions of the PDE system which exhibit an hyperbolic fixed point [11–13, 17]. This point corresponds to the right and left circular polarization states of the forward and backward beams, and plays the role of natural attractor for the system since any stationary trajectory will pass close to one of these two fixed points at the middle point of the fiber. Since for sufficient large coherence times, the spatio-temporal system follows approximately the stationary behavior, it explains therefore this unexpected polarization phenomenon, its robustness being connected to the geometric properties of the hyperbolic fixed point [11–13, 17]. This aspect is described in Fig. 4 which displays the evolution along the fiber of the stationary SOP in the  $z$ -direction. The stationary system described by Eq. (1) is a Liouville integrable system since it has as many constants of the motion as it has degrees of freedom. Using the LiouvilleArnold theorem, it can be shown that the states of this Hamiltonian lie on a two-dimensional torus. Some of the tori are not regular, but singular. It is the case of the torus with the two hyperbolic fixed points of the system, which is a doubly pinched torus (see Fig. 4 for a schematic representation). The pinched points of the torus correspond to the hyperbolic points [11–13].

#### IV. EXPERIMENTAL DEMONSTRATION

In order to study experimentally this effect of polarization organization, we have implemented the experimental setup depicted in Fig. 5. We consider uncorrelated fully

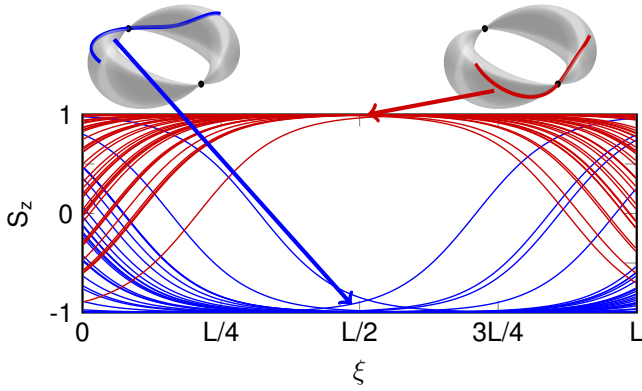


FIG. 4: (Color online) Stationary solutions  $S_z(\xi)$  along the fiber (the coordinate  $J_z(\xi)$  has exactly the same evolution in the stationary regime). The trajectories attracted towards the north and the south poles are respectively plotted in red (gray) and in blue (dark gray). The corresponding trajectories on the doubly pinched torus are schematically represented. The position of the two hyperbolic fixed points are indicated by a black dot.

polarized waves with a scrambling speed of a few Hz, which fully places the experiment in the quasi-stationary regime shown in Fig. 1 [14]. An optical fiber of 200 m

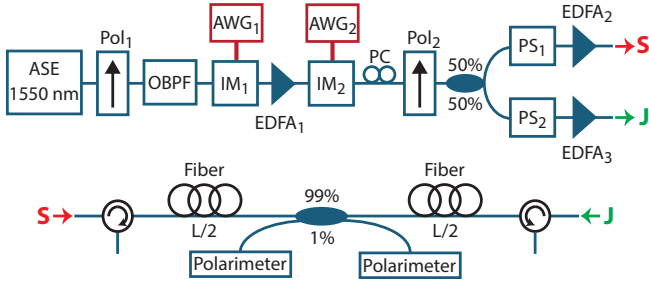


FIG. 5: (Color online) Experimental setup. ASE: amplified spontaneous emission, Pol: polarizer, OBPF: optical band-pass filter, IM: intensity modulator, AWG: arbitrary wave-form generator, EDFA: Erbium doped fiber amplifier, PS: polarization scrambler.

long segment is used as a nonlinear Kerr medium. The fiber under test is a Truewave HD fiber characterized by a chromatic dispersion parameter  $D = -14.5$  ps/km/nm, a nonlinear Kerr coefficient  $\gamma = 2.5$  W<sup>-1</sup>·km<sup>-1</sup> and linear losses of 0.2 dB/km. It is important to point out that, due to an optimized spinning process performed during the drawing stage, this kind of fiber presents a weak level of residual birefringence [3, 33]. Moreover, in order to prevent any additional source of birefringence, the fiber under study was first off-spooled and carefully wound around a 2-m diameter ring. In this way, the final 200-m long fiber segment can be considered as close as possible to the ideal isotropic case described above. Then, to

enable a direct monitoring of both counter-propagating SOP's, a 99:1 tap coupler was spliced at the exact middle point of the fiber. In addition, two circulators, implemented at each side of the fiber, allow to both inject the initial random waves and extract the final signals after the nonlinear propagation. Both  $S$  and  $J$  signals are generated from an Erbium-based spontaneous noise source (ASE) sliced into its spectrum domain by means of a 100-GHz optical bandpass filter and polarized thanks to an inline polarizer. Such a spectral linewidth enables to avoid any detrimental effect induced by stimulated Brillouin back-scattering within the fiber at power levels involved in the experiment. A series of two intensity modulators followed by Erbium amplifiers was then implemented to generate 4.5-W peak-power flat-top 5  $\mu$ s-pulses at a repetition rate of 5 kHz. We have also verified numerically that a duration of 5  $\mu$ s is sufficient for an incipient effect of polarization attraction with polarized waves, although several tens of  $\mu$ s are required to get a significant polarization with a saturation of the DOP growth for partially polarized beams. Furthermore, after the first stage of amplification (EDFA<sub>1</sub>), the signal was split into two identical replicas thanks to a 50:50 coupler in order to generate the two counter-propagating waves  $S$  and  $J$ . Finally, the initial SOP of both  $S$  and  $J$  were controlled independently and randomly by means of two polarization scramblers before the second stage of amplification (EDFA<sub>2</sub> and EDFA<sub>3</sub>).

Figure 6 displays the experimental recordings of the resulting Poincaré spheres of both  $S$  and  $J$  when the two waves are injected simultaneously at opposite ends of the fiber with a peak-power of 4.5 W. To this aim, 256 randomly distributed initial conditions were used for both waves as shown by the red dots covering the corresponding input spheres. In contrast, when monitored in the middle of the fiber, we can clearly observe that the SOPs of both  $S$  and  $J$  segregate around two pools of attraction, (here oriented along the  $z$  axis, following the theoretical model), thus demonstrating an efficient self-organization process between the two randomly polarized waves. Finally, as shown by the output sphere, beyond this mutual attraction process, both waves recover random polarization distributions at the fiber exit. The experimental results are in qualitative agreement with numerical simulations using the same counterpropagating waves.

To further assess the efficiency of this self-organization process, we have finally compared in Fig. 7 the probability density function of the three Stokes parameters  $S_x$ ,  $S_y$  and  $S_z$  of the  $S$  wave, respectively at the input and in the middle point of the fiber. These results confirm the expected behavior and show, in agreement with the numerical predictions of Fig. 3, that this process tends to focus the  $S_x$  and  $S_y$  Stokes parameters around the zero value, while segregating  $S_z$  around the two extrema  $\pm 1$ .

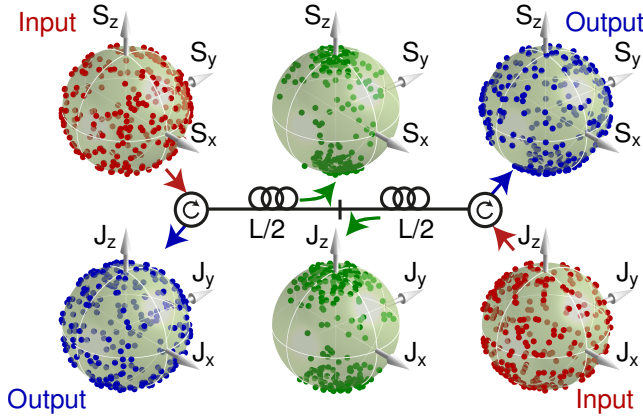


FIG. 6: (Color online) Experimental Poincaré spheres recorded for  $S$  and  $J$  at the input (red or gray dots), output (blue or dark gray dots) and in the middle of the fiber (green or light gray dots). The power of each wave is set to 4.5 W and the number of points is 256.

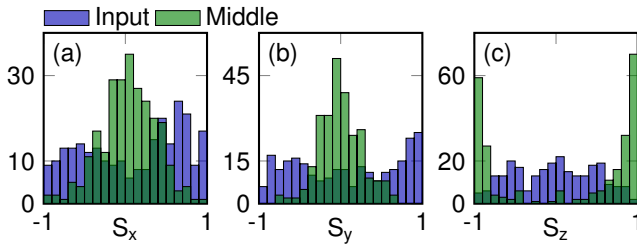


FIG. 7: (Color online) Experimental probability density function of the Stokes parameters for the  $S$  wave recorded at the input (blue or dark gray line) and in the middle of the fiber (green or light gray line). The power of each wave is set to 4.5 W and the number of points is 256.

## V. CONCLUSION AND PERSPECTIVES

In conclusion, we have investigated numerically and experimentally a novel phenomenon of polarization self-organization in which two uncorrelated partially polarized waves are injected at both ends of the fiber. For equal powers, the self-organization process occurs in the middle of the fiber. The two SOP are attracted toward the left or right circular polarizations states. The efficiency of the polarization process in terms of the coherence time of the partially polarized waves has been also characterized. One of the main interests of this phenomenon is its robustness in the sense that polarization attraction is observed over a large interval surrounding the middle point of the fiber. This remarkable effect of self-polarization has been identified in an isotropic fiber, which opens the way to a systematic investigation in other types of fibers such as randomly birefringent fibers used in optical telecommunications [14].

**Acknowledgments** We thank the Conseil Régional de Bourgogne Franche-Comté as well as the FEDER for their financial support. We are also very grateful to B. Sinardet and S. Pernot for the development of the electronic control part of our polarization scramblers.

- 
- [1] B. Rumpf, A.C. Newell, Phys. Rev. Lett. **87**, 054102 (2001).
  - [2] A. Picozzi, et al., Phys. Rep. **542**, 1 (2014).
  - [3] M. Gilles, P-Y. Bony, J. Garnier, A. Picozzi, M. Guasoni and J. Fatome, Nature Photonics, **11**, 102 (2017).
  - [4] D. J. Gauthier, M. S. Malcuit, A. L. Gaeta, and R. W. Boyd, Phys. Rev. Lett. **64**, 1721 (1990).
  - [5] S. Trillo and S. Wabnitz, Phys. Rev. A **36**, 3881 (1987).
  - [6] M. V. Tratnik and J. E. Sipe, Phys. Rev. A **35**, 2976 (1987).
  - [7] S. Pitois, G. Millot, and S. Wabnitz, Phys. Rev. Lett. **81**, 1409 (1998).
  - [8] D. David, D. D. Holm, and M. V. Tratnik, Phys. Rep. **187**, 281 (1990).
  - [9] S. Pitois, A. Picozzi, G. Millot, H. R. Jauslin, and M. Haelterman, Europhys. Lett. **70**, 88 (2005).
  - [10] S. Pitois, J. Fatome, and G. Millot, Opt. Express **16**, 6646 (2008).
  - [11] D. Sugny, A. Picozzi, S. Lagrange, and H. R. Jauslin, Phys. Rev. Lett. **103**, 034102 (2009).
  - [12] E. Assémat, S. Lagrange, A. Picozzi, H. R. Jauslin, and D. Sugny, Opt. Lett. **35**, 2025 (2010).
  - [13] E. Assémat, A. Picozzi, H. R. Jauslin and D. Sugny, J. Opt. Soc. Amer. B **29**, 159 (2012).
  - [14] V. V. Kozlov, J. Nuno, and S. Wabnitz, J. Opt. Soc. Am. B **28**, 100 (2011).
  - [15] E. Assémat, D. Dargent, A. Picozzi, H. R. Jauslin, and D. Sugny, Opt. Lett. **36**, 4038 (2011).
  - [16] V. Kozlov and S. Wabnitz, Opt. Lett. **35**, 3949 (2010).
  - [17] K. Hamraoui, M. Guasoni, A. Picozzi, E. Assémat, H. R. Jauslin, and D. Sugny, Phys. Rev. A **93**, 053830 (2016).
  - [18] J. Fatome, S. Pitois, P. Morin, and G. Millot, Opt. Express **18**, 15311 (2010).
  - [19] P. Morin, J. Fatome, C. Finot, S. Pitois, R. Claveau, and G. Millot, Opt. Express **19**, 17158 (2011).
  - [20] V. V. Kozlov, J. Fatome, P. Morin, S. Pitois, G. Millot, and S. Wabnitz, J. Opt. Soc. Am. B **28**, 1782 (2011).
  - [21] V. C. Ribeiro, R. S. Luis, J. M. D. Mendinueta, B. J. Put-



- tnam, A. Shahpari, N. J. C. Muga, M. Lima, S. Shinada, N. Wada, and A. Teixeira, *IEEE Photonics Technol. Lett.* **27**, 541 (2015).
- [22] A. DeLong, W. Astar, T. Mahmood, and G. M. Carter, *Opt. Express* **25**, 25625 (2017).
- [23] M. Barozzi and A. Vannucci, *J. Opt. Soc. Am. B* **30**, 3102 (2013)
- [24] M. Barozzi and A. Vannucci, *J. Opt. Soc. Am. B* **31**, 2712 (2014)
- [25] M. Barozzi and A. Vannucci, *Photonics Res.* **3**, 229 (2015)
- [26] J. Fatome, S. Pitois, P. Morin, D. Sugny, E. Assémat, A. Picozzi, H. R. Jauslin, G. Millot, V. V. Kozlov, and S. Wabnitz, *Sci. Rep.* **2**, 938 (2012).
- [27] P. Y. Bony, M. Guasoni, P. Morin, D. Sugny, A. Picozzi, H. R. Jauslin, S. Pitois and J. Fatome, *Nature Commun.* **5**, 4678 (2014)
- [28] P.-Y. Bony, M. Guasoni, E. Assmat, S. Pitois, D. Sugny, A. Picozzi, H. R. Jauslin, and J. Fatome, *J. Opt. Soc. Am. B* **30**, 2318 (2013)
- [29] G. D'Alessandro and W. J. Firth, *Phys. Rev. Lett.* **66**, 2597 (1991).
- [30] G. R. M. Robb, E. Tesio, G.-L. Oppo, W. J. Firth, and T. Ackemann, R. Bonifacio, *Phys. Rev. Lett.* **114**, 173903 (2015).
- [31] A. Picozzi, *Opt. Lett.* **29**, 1653, (2004).
- [32] A. Luis, *Phys. Rev. A* **71**, 053801 (2005).
- [33] T. Geisler, European Conference on Optical Communications (ECOC), Mo.3.3.1 (2006).